















The surface roughness ( $R_a$ ) values varying along the height of the sample ranged from 4.5 to 6.64 microns, while the hardness ranged from 24 Hv to 11 Hv in the aluminium samples.

Examining Fig. 6, it is seen that the variation of coefficient of friction with the axial force in both Al and steel powders lies on the same curve. Hence the frictional behaviour of the two materials seems to be very similar after a relatively large surface contact between the sample and the sleeve, indicating the overwhelming influence of the powder properties and forming conditions compared to the material on the development of coefficient of friction.

Despite the above, the frictional force between the cylindrical surfaces of the samples (compacted from aluminium or iron powder) and the tool are very different. The frictional force at large axial force is seen to rise rapidly in case of aluminium compared to that of iron (Fig. 7).

The area of contact depends strongly on the nature of the powder (Fig. 8). Aluminium being a more easily deformable (softer) material shows a greater area of contact compared to that in an iron powder compact. Powder morphology too has a strong influence on the interlocking among particles. Together with a greater yield strength, this explains a relatively lower contact area compared to that of aluminium.

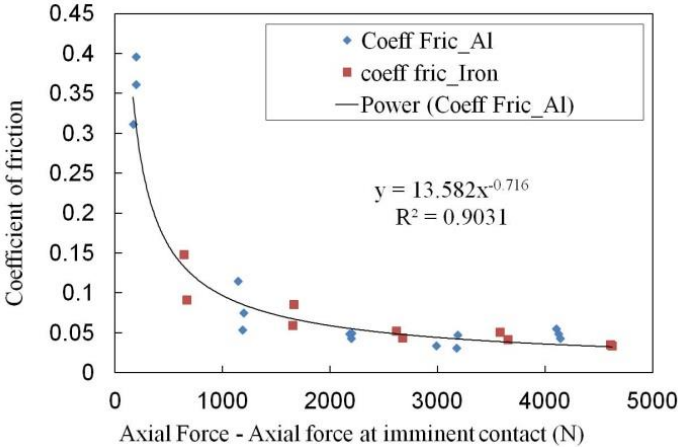


Fig. 6 Coefficient of friction with an increase in axial force for the two metal powders



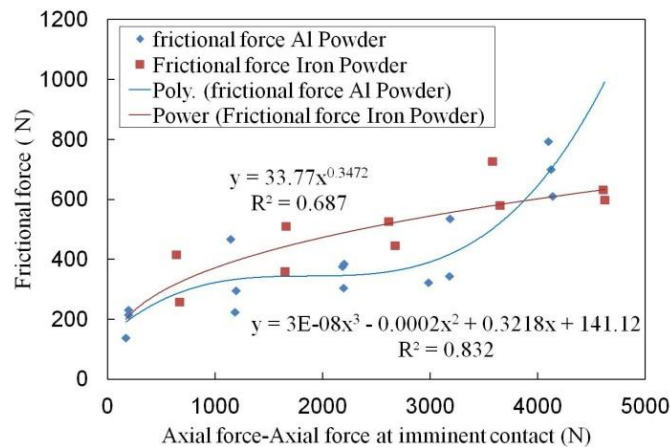


Fig. 7 Frictional force varying with axial force for powder compacts of iron and aluminium

Figs. 9(a)-(b) show the particle morphology for the aluminium powder (a) and the iron powder (b). Both the powders show a bimodal particle size, i.e., particles which can be divided into two classes - small sized particles and the large sized ones. The Al particles have a rounded shape and have well rounded edges, while those of iron are irregular in shape and show edges which are not rounded. This influences the interlocking among particles, and interparticle friction. Hence the compaction load increases without a significant increase in the percentage of area in contact with the sleeve. Besides, a relatively lower deformability of the iron particles leads to fragmentation of these particles under load.

Since the axial load after imminent contact would generate a normal contact force on the sleeve the magnitude of which would be subject to frictional resistance among particles, large scatter is observed in the variation frictional force with respect to the axial force for iron powder.

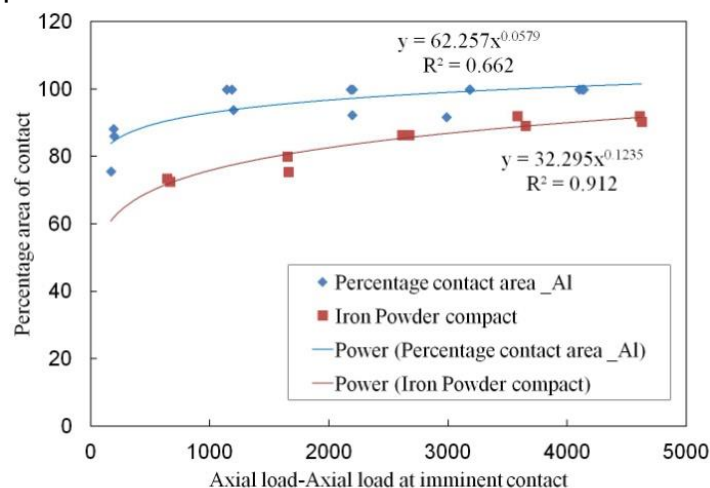


Fig. 8 Percentage area of contact with increasing axial load

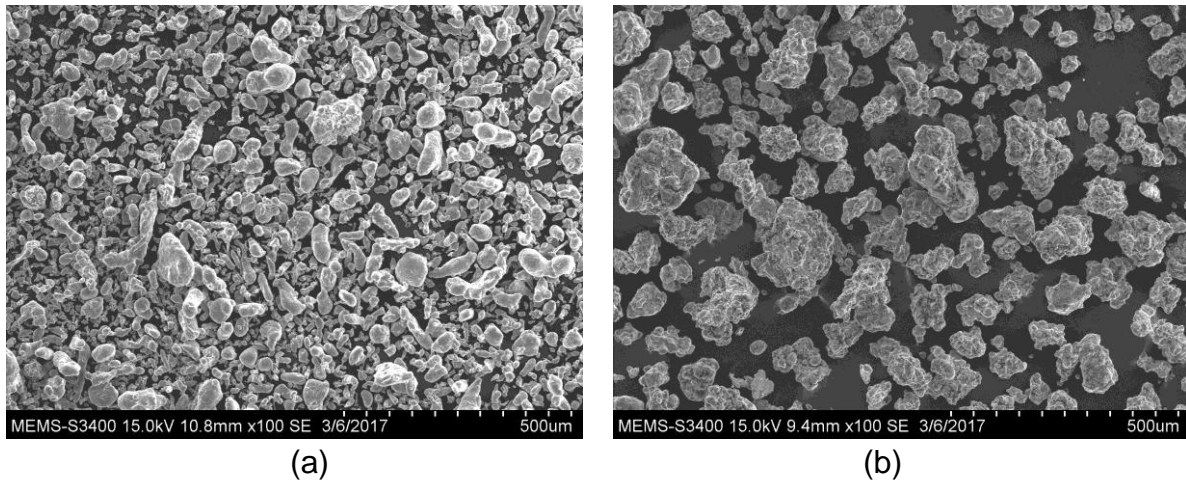


Fig. 9 Powder particle morphology of (a) Aluminium powder and (b) Iron powder used in the study

#### 4. CONCLUSIONS

From the foregoing observations and discussions, following conclusions emerge :

1. The various observations made on the basis of the axial friction test are well explained in light of results from the various investigations
2. The area of contact of the sample with the sleeve was always greater for aluminium powder compacts compared to those of iron powder.
3. The coefficient of friction decreases with an increase in the axial force, irrespective of the material.
4. The surface hardness after the friction test was found to be lower on account of removal of the hardened particles on the surface of the powder compacted samples.
5. The interface conditions at the room temperature strongly depend on the material of the powder, the particle morphology and the prior work hardening undergone by the particles.

#### Acknowledgements

The funding under the DST (INT/RUS/RFBR/P-214) for the experimental work conducted at IIT Bombay and RFBR (Project number 17-51-45085) Project is gratefully acknowledged.

#### References

- Alexandrov, S. (2005), "An Approach to Predicting Evolution of Material Properties Near Surfaces With High Friction in Metal Forming" In *World Tribology Congress III*, Washington, September.

- Alexandrov, S., Jeng, Y. R., and Hwang, Y. M. (2015), "Generation of a fine grain layer in the vicinity of frictional interfaces in direct extrusion of AZ31 alloy" *Journal of Manufacturing Science and Engineering*, Vol. **137**(5), 1-9.
- Hora, P., Gorji, M., and Berisha, B. (2012), "Modeling of friction phenomena in extrusion processes by using a new torsion-friction test" *Key Engineering Materials*, Vol. **491**, 129-135.
- Lyamina, E., Alexandrov, S., Grabco, D., and Shikimaka, O. (2007), "An approach to prediction of evolution of material properties in the vicinity of frictional interfaces in metal forming" *Key Engineering Materials*, Vol. **345**, 741-744.
- Sanabria, V., Mueller, S., and Reimers, W. (2014), "A new high speed friction test for extrusion processes", *Key Engineering Materials*, Vol. **585**, 33-39.
- Sanabria, V., Mueller, S., and Reimers, W. (2014), "Microstructure evolution of friction boundary layer during extrusion of AA 6060", *Procedia Engineering*, **81**, 586-591, 11th International Conference on Technology of Plasticity, Nagoya.
- Sanabria, V., Mueller, S., Gall, S., and Reimers, W. (2014), "Investigation of friction boundary conditions during extrusion of aluminium and magnesium alloys" *Key Engineering Materials*, Vol. **611**, 997-1004.